Study of the onset of neoclassical tearing modes at the ASDEX Upgrade tokamak

S. Fietz, M. Maraschek, H. Zohm, L. Barrera, R. M. McDermott,
M. Reich and the ASDEX Upgrade Team
Max-Planck-Institut für Plasmaphysik, Boltzmannstraße 2, 85748 Garching, Deutschland

1. Introduction

Neoclassical tearing modes (NTM) are one of the most serious performance limiting instabilities in a fusion devices like ITER. NTMs are destabilised as a consequence of a seed perturbation and are driven by a loss of helical bootstrap current inside the island. The appearance of these instabilities is accompanied with a loss of confined plasma energy. Additionally, these modes can stop the plasma rotation, lock to the vessel wall, flush out all plasma energy and terminate a discharge. In ITER the confinement reduction will limit the achievable fusion power, whereas a disruption is likely to damage the vessel wall. One key issue is the rotation dependence of NTMs, especially at the NTM onset. ITER will be operated at low plasma rotation, which is different from most present day experiments. No theory is currently available to describe this dependence. Experiments are therefore required to provide a basis for the theory to describe the physics. Additionally from the experiments scalings can be developed and extrapolated in order to predict the NTM behaviour in the parameter range relevant for ITER.
There exist several possibilities how plasma rotation can influence the NTM behaviour. It has been proposed that changes in rotation or rotation shear can reduce the normally stabilising effect of the classical tearing stability index Δ' [1]. Rotation can also influence the stability of NTMs by means of small island effects, via e.g. the ion polarisation current [2] [3]. A further important issue is the effect of rotation on the trigger mechanism. Finally, rotation can influence the island stability due to changes of the impact of error fields on the island.
At DIII-D [4] and NSTX [5] it was found that with decreasing co-rotation or rotation shear the NTM onset threshold decreases and that the role of rotation shear on the NTM stability is more important than that of rotation alone. At DIII-D it is shown that the NTM onset threshold decreases further with increasing counter-rotation. Similarly, for decreasing rotation shear, the onset threshold decreases continuously also when entering the region of negative shear, which is related to counter-rotation. This raised the question of whether a sign effect is responsible for the different behaviour with co- and counter-rotation or if the minimum onset threshold is shifted towards negative rotation which would indicate that an "offset" exists. If this is the case, then it is possible that this minimum in rotation has not been reached yet at DIII-D and even stronger counter-rotation data are needed to cross this minimum. In the following the corresponding results from ASDEX Upgrade (AUG) for the (3,2) [6] and (2,1) NTM onset which differ in some respects from those at DIII-D and NSTX are presented.

2. Experimental approach

The growth of an NTM can be described by the modified Rutherford equation [7] [8]. Beside the classical tearing stability index Δ', the destabilising effect of the bootstrap current and several small island effects, which are responsible for the need of a trigger perturbation, alter the stability of an NTM. A simple and commonly used expression for the perturbation of the bootstrap current inside an island is $\delta j_{\mathrm{BS}} \approx -\varepsilon^{\frac{1}{2}} \nabla p / B_{\mathrm{pol}} \approx \beta_{\mathrm{pol}} / L_{\mathrm{p}}$.
In the experimental analysis, we distinguish between different trigger mechanisms which, due to magnetic coupling, induce a seed island at the resonant surface. Each onset point is clearly correlated with a distinct trigger mechanism. For most of the discharges the trigger mechanism could be identified unmistakably as either an ELM, a fishbone or a sawtooth crash. Cases,

where the mode grows without any visible trigger are also common. For six NTM onsets (1,1) activity was observed but the trigger mechanism could not be specified. In cases where at the mode onset multiple events took place the trigger mechanism is labelled as 'unclear'. At AUG the (m,n)=(3,2) and (2,1) NTMs are the most common and hence a large data set of NTM onset points with a wide range of plasma rotation is available. To extend the database, especially in the low rotation regime and with counter-rotation, dedicated experiments have been carried out, with varying heating power and external torque input, using different combinations of wave heating (ECRH and ICRH) and neutral beam injection (NBI). In normal operation the NBI is oriented in the co-direction relative to the plasma current. Experiments with counter-rotation were done by reversing the plasma current and the magnetic field direction. With this the NBI is oriented in the counter-direction. These experiments were limited in NBI heating power due to impurity influx created by first orbit losses. As a consequence the range of achievable counter-rotation was limited. For the following investigations all parameters are taken at the location of the magnetic island. The detailed evaluation is mainly based on the (3,2) NTMs due to its significantly larger database. For the (2,1) NTM in many cases the onset conditions are unclear and hence the accurately analysable database is smaller.

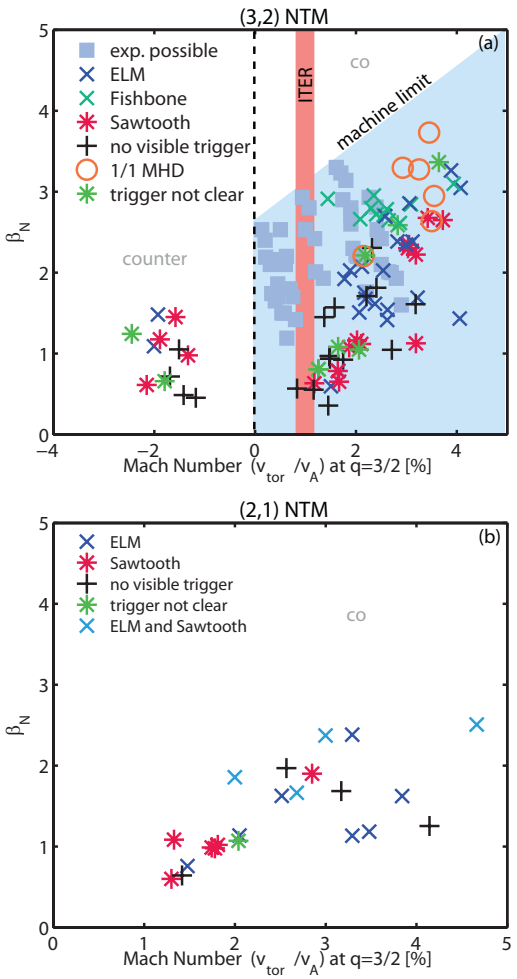

Figure 1: Normalised β_N at the onset of (a) (3,2) and (b) (2,1) NTMs versus Ma_A at r_{res}. The symbols indicate the different trigger mechanisms. In (a) the blueish grey boxes indicate the experimentally possible data range, the upper bound is indicated as machine limit.

3. Experiment results

In this section the influence of the toroidal rotation velocity on the NTM onset threshold is investigated. Similar to studies at other devices in the following, the rotation velocity is normalised to the Alfvén velocity ($v_A = B_{tor}/\sqrt{\mu_0 n_i m_i}$), with B_{tor} the toroidal magnetic field, n_i the ion density, m_i the ion mass and μ_0 the magnetic vacuum permeability), due to the only marginal dependence of the NTM onset threshold on toroidal rotation alone. This normalised quantity is then defined as Ma_A (Alfvén Mach number).

In figure 1 the global β_N at the NTM onset is plotted against the normalised rotation for the (3,2) NTMs in (a) and the (2,1) NTMs in (b). Also indicated in 1 (a) is the hypothetical achievable parameter range in β_N and Ma_A, which is estimated assuming a momentum confinement time equal to the energy confinement time and an H_{98}-factor of one. In this calculation the plasma rotation was varied by including different mixtures of the heating methods (NBI max. 20 MW and wave heating max. 10 MW) available at AUG. These calculated data points, which are shown as grey-blue boxes, indicate the hypothetical experimentally achievable data range for the given heating power at AUG without NTM. The upper bound is marked as machine limit.

In figure 1 (a) the β_N at the NTM onset linearly increases with increasing Ma_A for co- and counter-rotation. This is more distinct for the co-rotation data, but however the trend

is also visible for counter-rotation. Latest evaluation confirm the trend for co-rotation also for the (2,1) onset (fig. 1 (b)). Unfortunately no counter-rotation data are available for the (2,1) NTM onset. Additionally, it is clearly visible for the (3,2) NTM dataset that the NTMs limit the maximal achievable β_N and hence limit the plasma operation below the machine limit. Heating with NBI not only increases the β_N but also exerts a torque on the plasma and hence increases plasma rotation at the same time. The fact that the machine limit is higher than the achievable β_N then also indicates that this linear dependence of the β_N and the rotation velocity at the NTM onset is not trivial.

Considering that the NTM onset threshold is described more accurately by the perturbation of the bootstrap current inside the island, another analysis method using local parameters is shown in figure 2 (a) for the (3,2) NTM onset. In this plot additional data points from different discharges where no NTM is present are included. An upper NTM onset threshold is clearly visible in this analysis, which linearly increases with Ma_A in the region of high rotation. All of the data points, including the NTM onset data and the data without NTMs, are situated below this threshold in the metastable region. This means that plasma operation is ultimately limited by NTMs when this threshold is reached and that the region above this threshold cannot be realised in experiment. This is different when the resonant q-surface is not present or the NTM is actively stabilised.

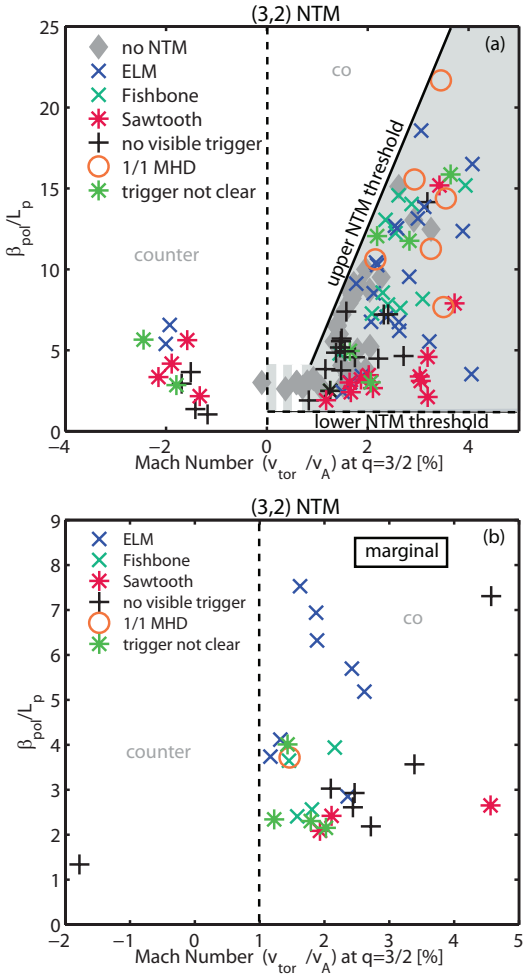

Figure 2: (a) (3,2) NTM threshold at the onset (a) and the marginal point (b) versus Ma_A at r_{res}. The symbols indicate the different trigger mechanisms or data points without NTMs

The lower NTM threshold, which defines the minimum required drive for the occurrence of an NTM and can in principle be explained by the Rutherford equation, does not to depend on rotation. In the region of low normalised rotation (Ma_A<1), where the intersection of the upper and lower threshold should be, the upper threshold seems not to depend on rotation anymore. In this region of low rotation the discharges are mainly heated by wave heating, which appears to change the NTM stability behaviour or the trigger mechanisms and blurs the boundaries. The scatter of the NTM onset data in the metastable region (grey coloured area) is caused by the different trigger events. The trigger process is different for every NTM onset, even if the triggering instability is the same, and hence leads to different seed island sizes and in consequence different onset thresholds.

Although the counter-rotation data is limited, also with this analysis method a trend towards increasing co- and counter-rotation with increasing NTM onset threshold is visible, which leads to a minimum threshold in the region of zero rotation. For co-rotation this trend can also be seen for all of the different trigger sub-sets. This disagrees with the experiments at DIII-D, where a further decrease of the onset threshold with counter-rotation was found. This discrepancy could be explained by an offset in the DIII-D data e.g. caused by the ion diamagnetic drift frequency.

Since for the AUG data the ion diamagnetic drift frequency is small compared to DIII-D, we expect to have no obvious offset of the threshold minimum in figure 2 (a).
When plotting the NTM onset threshold against Ma_A it is noteworthy that in the region of low rotation NTMs are mostly triggered by a sawtooth crash or appear without any trigger. This can be seen in figures 1 (a)+(b) and 2 (a). It is well known that a sawtooth crash can lead to a strong perturbation at the resonant surface and this results in a low NTM threshold. In contrast, based on the fact that the triggerless case is seen as the weakest trigger mechanism, one would expect these cases to have a higher onset threshold. From this discrepancy one can infer that there exists an influence of plasma rotation on the underlying tearing stability. This means that at lower plasma rotation the Δ'-term changes such that the plasma is less stable against NTMs as already proposed in [4] and [1]. To disentangle the influence of rotation on the island stability itself as opposed to the trigger mechanism the NTM behaviour at the marginal point was investigated for the (3,2) NTMs (fig. 2 (b)). So far no dependence is observed at the marginal point, which could indicate that the rotation dependence at the onset is caused by an impact of rotation on the trigger mechanism.
Further, studies on the influence of the differential rotation between the trigger and the mode surface on the NTM onset have been done. These studies indicate that the NTM onset threshold increases with differential rotation for the ELM and fishbone triggered cases whereas no dependence on differential rotation is seen for the sawtooth triggered cases. This means that ELMs and fishbones can more easily lead to a sufficiently large perturbation at the resonant surface when the rotation profile is flat, whereas for sawtooth crashes the rotation profile seems to have no impact on the triggering mechanism. This is an indication that the magnetic reconnection forced by a sawtooth crash at the resonant surface is strong enough to induce a sufficiently large seed island independent of the rotation profile. This is also in line with the observation that NTMs triggered by a sawtooth crash can appear at a low onset threshold.

3. Conclusion

The work presented here shows that the NTM onset threshold increases with increasing co- and counter-rotation. Hence, the NTM onset behaviour does not depend on the direction of the plasma rotation and NTMs can more easily be triggered at low plasma rotation. The region of minimum onset threshold could be reached and the trend with counter-rotation clearly verified, contrary to DIII-D. The formation of an upper NTM onset threshold in local parameters is observed. This upper onset threshold increases with increasing normalised plasma rotation but is less distinct at low plasma rotation. This indicates that the NTM behaviour changes at low rotation. The observation that the triggerless cases appear mainly at low rotation further confirms this. At low normalised rotation Δ' is less stabilising, and hence, the equilibrium current profile appears to be different. In contrast, at the marginal point, shortly before the mode disappears and the trigger process plays no role anymore, no dependence is observed so far. This indicates that the dependence on rotation at the onset is caused by an influence of rotation on the trigger mechanism. Additionally, steeper rotation profiles seem to hamper the appearance of NTMs. In addition, high differential rotation appears to impede the triggering process for ELMs and fishbones as a trigger, but not for sawtooth crashes.

This project has received funding from the Euratom research and training programme 2014-2018

References

[1] R. J. La Haye et al., PoP **17** 2010)
[2] F. L. Waelbrock et al., PRL **87** (2001)
[3] H. R. Wilson et al., PPCF **38** (1996)
[4] R. J. Buttery et al., PoP **15** (2008)
[5] S. Gerhardt et al., NF **49** (2009)
[6] S. Fietz et al., PPCF **55** (2013)
[7] P. H. Rutherford, PoF **16** (1973)
[8] O. Sauter et al., PoP **4** (1997)